

# SCIENTIFIC REPORTS



OPEN

## Molecular mechanisms underlying the involvement of the sigma-1 receptor in methamphetamine-mediated microglial polarization

Jie Chao<sup>1,2</sup>, Yuan Zhang<sup>1</sup>, Longfei Du<sup>1</sup>, Rongbin Zhou<sup>3</sup>, Xiaodong Wu<sup>1</sup>, Kai Shen<sup>4</sup> & Honghong Yao<sup>1,5</sup>

Our previous study demonstrated that the sigma-1 receptor is involved in methamphetamine-induced microglial apoptosis and death; however, whether the sigma-1 receptor is involved in microglial activation as well as the molecular mechanisms underlying this process remains poorly understood. The aim of this study is to demonstrate the involvement of the sigma-1 receptor in methamphetamine-mediated microglial activation. The expression of  $\sigma$ -1R, iNOS, arginase and SOCS was examined by Western blot; activation of cell signaling pathways was detected by Western blot analysis. The role of  $\sigma$ -1R in microglial activation was further validated in C57BL/6 NWT and sigma-1 receptor knockout mice (male, 6–8 weeks) injected intraperitoneally with saline or methamphetamine (30 mg/kg) by Western blot combined with immunostaining specific for Iba-1. Treatment of cells with methamphetamine (150  $\mu$ M) induced the expression of M1 markers (iNOS) with concomitant decreased the expression of M2 markers (Arginase) via its cognate sigma-1 receptor followed by ROS generation. Sequential activation of the downstream MAPK, Akt and STAT3 pathways resulted in microglial polarization. Blockade of sigma-1 receptor significantly inhibited the generation of ROS and activation of the MAPK and Akt pathways. These findings underscore the critical role of the sigma-1 receptor in methamphetamine-induced microglial activation.

Methamphetamine has a highly addictive effect on the central nervous system (CNS) and is abused throughout the world<sup>1,2</sup>. Methamphetamine abuse through acute and chronic use is a serious public health problem because of its adverse effects, which include hyperthermia, disruption of the blood-brain barrier, edema and cognitive impairment<sup>3,4</sup>. Currently, the US Food and Drug Administration (FDA) has yet not approved any pharmacological treatment for psychostimulant dependence, and an effective method of overcoming the negative effects of methamphetamine is urgently needed.

Microglia are resident immune cells and are involved in innate inflammatory responses within the CNS<sup>5</sup>. Microglia are known to be actively involved in various neurological diseases, such as Parkinson's disease<sup>6</sup>, stroke<sup>7</sup> and depression<sup>8</sup>. Accumulating evidence suggests that methamphetamine-induced neurotoxicity is associated with microglial activation<sup>9</sup>, and activated microglia are thought to participate in either pro-toxic or protective mechanisms in the brain<sup>10–12</sup>. The classic M1 and alternative M2 phenotypes, which are the two most polarized phenotypes, represent two extremes of a dynamic changing state of microglial activation. M1 and M2 microglia can be distinguished through their expression of a panel of functional and phenotypic markers<sup>13</sup>. 'M1-like' activation is characterized by the expression of potent pro-inflammatory mediators such as TNF- $\alpha$  and inducible nitric oxide synthase (iNOS) and is associated with substantial tissue damage. In contrast, 'M2-like' activation is associated with the increased secretion of neurotrophic factors and expression of the enzyme arginase 1, which plays

<sup>1</sup>Department of Pharmacology, Medical School of Southeast University, Southeast University, Nanjing, China.

<sup>2</sup>Department of Physiology, Medical School of Southeast University, Southeast University, Nanjing, China. <sup>3</sup>Institute of Immunology and the CAS Key Laboratory of Innate Immunity and Chronic Disease, School of Life Sciences and Medical Center, University of Science and Technology of China, Hefei, China. <sup>4</sup>Department of Pharmacy, Nantong Tongzhou People's Hospital, Nantong, China. <sup>5</sup>Institute of Life Sciences, Key Laboratory of Developmental Genes and Human Disease, Southeast University, Nanjing, China. Correspondence and requests for materials should be addressed to K.S. (email: [1107577390@qq.com](mailto:1107577390@qq.com)) or H.Y. (email: [yaohh@seu.edu.cn](mailto:yaohh@seu.edu.cn))

a vital role in wound healing<sup>14,15</sup>. Modulation of microglial phenotype is a well-known and appealing neurotherapeutic strategy, but the molecular mechanisms that drive the methamphetamine-induced switch in microglial phenotype remain poorly understood.

Sigma receptors are classified into two subtypes, sigma-1 and sigma-2 receptors<sup>16</sup>. The sigma-1 receptor, which is a unique ligand-regulated molecular chaperone, is related to many conditions, such as stroke<sup>17</sup>, pain<sup>18</sup> and HIV infection<sup>19</sup>. The sigma-2 receptor plays a role in pathogenesis by modulating cell proliferation<sup>20</sup>. Earlier studies have also suggested that methamphetamine exhibits significant affinity for the sigma-1 receptor. For example, BD1047, a specific inhibitor of the endoplasmic membrane-bound sigma-1 receptor, reduces neuronal injury in the methamphetamine-exposed hippocampus<sup>21</sup>. A recent study also reported that sigma-1 receptor antagonists attenuate methamphetamine-induced hyperactivity and neurotoxicity<sup>22</sup>. Although the close relationship between the sigma-1 receptor and methamphetamine has been the focus of extensive pharmacological studies, genetic evidence to further elucidate the role and mechanisms of sigma-1 receptor signaling in methamphetamine-mediated microglia activation is still missing.

In the current study, we demonstrate the molecular mechanisms underlying methamphetamine-induced phenotypic changes with a focus on the sigma-1 receptor. This study not only elucidates the cellular signaling mechanisms that underlie methamphetamine-mediated microglial activation but also sheds light on novel therapeutic targets that could be exploited to treat neuroinflammation.

## Materials and Methods

**Reagents.** Methamphetamine was purchased from the National Institute for the Control of Pharmaceutical and Biological Products (Beijing, China). The specific MEK1/2 inhibitor U0126, JNK inhibitor SP600125, p38 inhibitor SB203580 and phosphatidylinositol-3 kinase (PI3K) inhibitor LY294002 were purchased from Calbiochem (San Diego, CA). The NADPH inhibitor apocynin was obtained from Sigma-Aldrich (St. Louis, MO, USA), and the STAT3 inhibitor statin was ordered from Selleck (Houston, TX, US). The concentrations of these inhibitors were based on a concentration-curve study and our previous reports<sup>23</sup>.

**Animals.** C57BL/6N mice (male, 6–8 weeks) were purchased from the Comparative Medicine Centre, Yangzhou University (Yangzhou, China). Sigma-1 receptor knock out (KO) mice were originally obtained from the Laboratory Animal Center of University of Science and Technology of China (Hefei, China) and were backcrossed 10 generations to a C57BL/6N inbred background. All of the animals were housed under conditions of constant temperature ( $22 \pm 1^\circ\text{C}$ ) and humidity, with a 12 h light (between 8:30 and 20:30)/12 h dark cycle and free access to food and water. After the animals were habituated, the mice were injected i.p. with methamphetamine (30 mg/kg) every 2 h for a total of four injections. Another group of mice received escalating dose methamphetamine. As described in our previous studies<sup>24</sup>, the mice were injected intraperitoneally with incrementally increasing doses on alternating days (i.p. 1.5 mg/kg on days 1–2, once a day; 4.5 mg/kg on days 3–4, once a day; 7.5 mg/kg on days 5–6, once a day; and 10 mg/kg on days 7–8, every 2 h for a total of four times a day). Thirty minutes or twenty-four hours after the last injected, the mice were euthanized and different brain regions were dissected for further analysis of phosphorylation of MAPK/Akt pathways or the expression of iNOS, Arginase and SOCS3, respectively. The control group was injected with saline in the same volume that was used for the methamphetamine treatments. All animal procedures were performed according to the Guidelines of Accommodation and Care for Animals formulated by the Chinese Convention for the Protection of Vertebrate Animals Used for Experimental and Other Scientific Purposes of Southeast University.

**Cell culture.** Postnatal (P1 to P3) C57BL/6N mice were purchased from the Comparative Medicine Centre, Yangzhou University (Yangzhou, China). After the membranes and large blood vessels were removed using gauze, dissociated brain tissues were digested with Trypsin-EDTA. The cells were plated in poly-L-lysine-coated cell culture flasks in Dulbecco's modified Eagle's medium (DMEM) containing 10% heat-inactivated fetal bovine serum (FBS) and 1% penicillin/streptomycin. The medium was changed for the first time after the cells were allowed to attach for three days. Beginning seven days later, the medium was replaced every 3 days with fresh medium containing 0.25 ng/ml granulocyte/macrophage colony-stimulating factor (GM-CSF) to promote microglia proliferation. The microglia were detached from the flasks by shaking and collected by centrifugation ( $1500\text{g} \times 5\text{min}$  at  $4^\circ\text{C}$ ).

BV-2 immortalized cells were purchased from the China Center for Type Culture collection (Wuhan, China) and were cultured in DMEM supplement with 10% FBS and 1% penicillin/streptomycin and incubated at  $37^\circ\text{C}$  in a humidified atmosphere of 5%  $\text{CO}_2$  and 95% air. The BV-2 cells were used up to passage 20.

**Lentiviral transduction of BV-2 with RFP.** BV-2 cells were transduced using LV-RFP lentiviruses (Hanbio Inc., Shanghai, China) as previously described<sup>25,26</sup>. Briefly, P3–4 BV-2 cells were cultured in 24-well plates at  $1 \times 10^4$  cells/well in 10% FBS in DMEM for 48 h. The medium was then replaced with 1 ml of fresh medium and 8  $\mu\text{g/ml}$  polybrene. Then, 100  $\mu\text{L}$  of lentivirus solution ( $10^7$  IU/ml) was added to each well, and the cells were incubated at  $37^\circ\text{C}$  in 5%  $\text{CO}_2$  for 24 h. After the incubation period, the treatment medium was replaced with fresh 10% FBS in DMEM, and the cells were cultured at  $37^\circ\text{C}$  in 5%  $\text{CO}_2$  until they reached >50% confluence. Transduced cells were selected using blasticidin as follows: the medium was replaced with 10  $\mu\text{g/ml}$  puromycin and 10% FBS in DMEM, and the cells were cultured at  $37^\circ\text{C}$  in 5%  $\text{CO}_2$  for 24 h. The cells were then washed twice with fresh 10% FBS in DMEM.

**Reactive oxygen species (ROS) assay.** BV-2 cells transduced with RFP-lentivirus were treated with methamphetamine in a time-dependent manner or were pretreated with BD1047 for one h and then treated with methamphetamine. The BV-2 cells were then stained for 30 min with 10  $\mu\text{M}$  carboxy-H2DCFDA (Molecular Probes, Eugene, OR); 1  $\mu\text{M}$  Hoechst 33342 (Molecular Probes, Eugene, OR) was added during the last 5 min of the

incubation. After the incubation, the cells were washed with PBS and then immediately visualized using a fluorescence microscope (Zeiss, Göttingen, Germany) or resuspended in PBS containing 20 mM glucose before being analyzed with a Synergy fluorescence plate reader (Bio-Tek Instruments, Winooski, VT). The DCF fluorescence values were divided by the corresponding Hoechst fluorescence values for normalization.

**Western blot.** For protein isolation from brain tissue, different brain regions were dissected from mice treated with methamphetamine and homogenized with the lysis buffer according to the manufacturer's instructions. For cell culture, the BV-2 cells were also lysed with the Mammalian Cell Lysis Kit (Sigma-Aldrich, St. Louis, MO, USA). For Nuclear protein extraction, nuclear lysates were isolated using the NE-PER Nuclear and Cytoplasmic Extraction Kit (Pierce, Rockford, IL, USA) according to the manufacturer's instructions. Briefly, treated BV-2 cells were harvested with trypsin-EDTA and centrifuged at 500Xg for 5 min followed by wash with PBS. After centrifuge at 500Xg for 3 min, the cell pellet was resuspended in ice-cold cytoplasmic extraction reagent I with protease inhibitors and incubated on ice for 10 min. Then ice-cold cytoplasmic extraction reagent II was added to the cell suspension and incubated on ice for 1 min with vortex on the highest setting. Once the cytoplasmic portion of the cells was purified, nuclear extraction followed using nuclear extraction reagent containing protease inhibitors.

After protein extraction, the total protein concentration was assessed using the Bradford assay and equal protein samples were loaded on a 12% polyacrylamide gel and transferred to polyvinylidene difluoride membranes, which were then incubated with a blocking buffer containing 5% non-fat dry milk in Tris-buffered saline with Tween-20. The membranes were then incubated with primary antibodies for p-ERK/ERK, p-JNK/JNK, p-p38/p38, p-Akt/Akt, suppressor of cytokine signaling 3 (SOCS3) (Cell Signaling, 1:1000), signal transducer and activator of transcription 3 (STAT3) (Proteintech, 1:1000), iNOS (Abcam, 1:1000) and  $\beta$ -actin (Santa Cruz, 1:500) as previously described<sup>27,28</sup>.

**Statistical analysis.** Statistical analysis was performed using SigmaPlot software (SigmaPlot 11.0, Systat, Inc). The data are expressed as the mean  $\pm$  SD, and experiments were independently repeated at least three times. The significance of differences between the control samples and those treated with various drugs was tested by one-way ANOVA, with Tukey or Bonferroni correction for multiple comparisons. Values of  $p < 0.05$  were considered significant.

## Results

### Involvement of the sigma-1 receptor in methamphetamine-mediated microglial polarization.

Although recent studies have suggested that BV-2 cells express the sigma-1 receptor, which interacts with methamphetamine at physiologically relevant concentrations<sup>29</sup>, very little is known about the role of the sigma-1 receptor in methamphetamine-mediated microglial polarization. According to our previous study<sup>30</sup>, 150  $\mu$ M was the optimal dose of methamphetamine to induce glial activation. To assess the time course of methamphetamine's effects, BV-2 cells were exposed to 150  $\mu$ M for varying time periods. Treating microglia with methamphetamine increased iNOS expression, however, methamphetamine significantly down-regulated the expression of the anti-inflammatory markers arginase and SOCS3 (Fig. 1A). These findings were also reproduced in primary microglia (Fig. 1B). We next wanted to assess whether the sigma-1 receptor was involved in the methamphetamine-induced phenotypic changes in BV-2 cells. Pretreating BV-2 cells with the sigma-1 receptor antagonist BD1047 for 1 h followed by incubation with methamphetamine for 12 h significantly reduced the methamphetamine-induced increased the ratio of M1 marker (iNOS) and M2 marker (arginase) (Fig. 1C,D). Taken together, these findings clearly demonstrate that the sigma-1 receptor plays a critical role in methamphetamine-induced microglial polarization.

**Methamphetamine induced ROS generation.** While the role of oxidative stress in methamphetamine-induced dopaminergic neurotoxicity is well known<sup>31</sup>, the role of ROS in the mechanisms underlying sigma-1 receptor-mediated modulation of microglial phenotype remains unclear. First, we examined the effect of methamphetamine on the formation of ROS. BV-2 cells exposed to methamphetamine for varying amounts of time exhibited an increase in ROS generation, with a peak at 15 min (Fig. 2A). Since we have determined that ROS also play a crucial role in microglial polarization, we next want to investigate whether there is a link between the sigma-1 receptor and the generation of ROS using a pharmacological approach. Interestingly, pretreating BV-2 cells with BD1047 for 1 h abrogated the methamphetamine-induced ROS formation (Fig. 2B), this was further validated by fluorescence microscope (Fig. 2C). Consistent with the role of the sigma-1 receptor in microglial polarization, in BV-2 cells that were pretreated for 1 h with the NADPH oxidase inhibitor apocynin, differentiation from the anti-inflammatory M2 phenotype to the inflammatory M1 phenotype was also significantly suppressed (Fig. 2D,E).

**Methamphetamine induced activation of the MAPK and PI3K/Akt pathways.** Several studies have implicated the role of the MAPK and PI3K/Akt pathways in methamphetamine-mediated signaling<sup>32-34</sup>. Treating BV-2 cells with methamphetamine transiently increased the phosphorylation of ERK, JNK, and p38 MAPKs, with a peak at 15 or 60 min (Fig. 3A). Methamphetamine exposure also activated Akt in a time-dependent manner, with maximal activation at 5 min (Fig. 3A). Because sigma-1 receptor-mediated ROS generation and signaling pathway activation are both critical processes that are involved in microglial polarization, we sought to investigate the presence of a link that could tie together the formation of ROS and the signal transduction pathways using a pharmacological approach. BV-2 cells were pretreated with the sigma-1 receptor antagonist-BD1047 or the NADPH oxidase inhibitor-apocynin and then treated with methamphetamine, and activation of the MAPK and PI3K/Akt pathways was assessed. As shown in Fig. 3B,C, pretreatment of cells with BD1047 or apocynin significantly inhibited activation of the MAPK and PI3K/Akt pathways induced by methamphetamine. To better understand the effect of methamphetamine on the activation of the MAPK and PI3K/

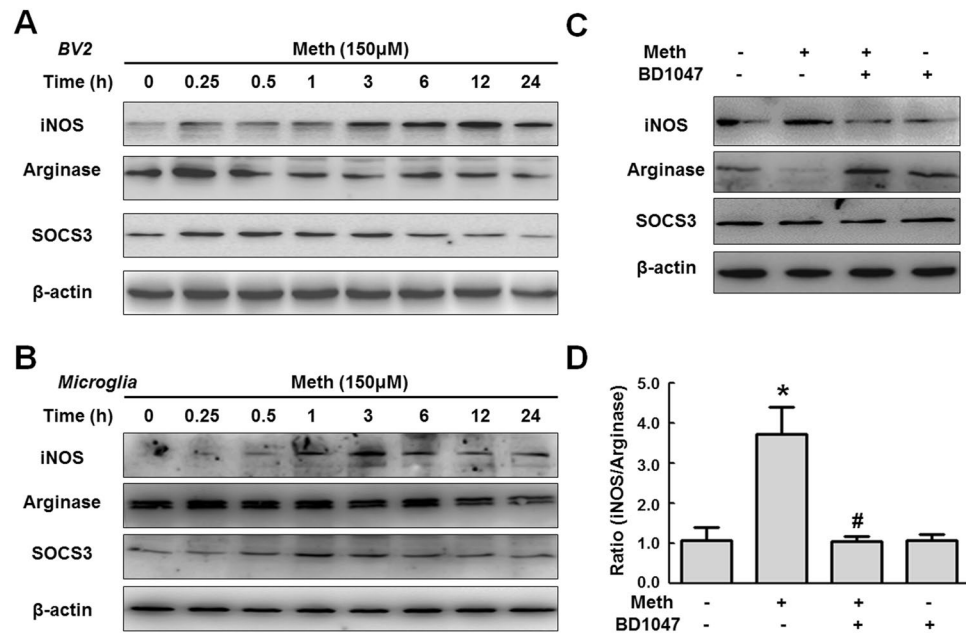


**Figure 1.** Involvement of the sigma-1 receptor in methamphetamine-mediated microglial polarization. **(A)** Representative western blot showing the effects of methamphetamine (150  $\mu$ M) on the expression of the M1 polarization markers iNOS, arginase and SOCS3 in BV-2 cells. **(B)** Representative western blot showing the effects of methamphetamine (150  $\mu$ M) on the expression of the M1 polarization markers iNOS, arginase and SOCS3 in microglia. **(C)** Representative western blot showing the effects of the sigma-1 receptor inhibitor BD1047 on the methamphetamine-induced expression of iNOS, arginase and SOCS3 in BV-2 cells. **(D)** Densitometric analyses for five separate experiments suggest that methamphetamine induced the ratio of M1 marker (iNOS) and M2 marker (arginase), which was attenuated by BD1047 pretreatment. \* $p < 0.05$  vs the control group; # $p < 0.05$  vs the Meth-treated group using one-way ANOVA. Meth, methamphetamine.

Akt pathways, mice were intraperitoneally injected with methamphetamine (30 mg/kg) every 2 h for a total of four injections (Fig. 3D) or with escalating dose methamphetamine (1.5 mg/kg, 4.5 mg/kg, 7.5 mg/kg, and 10 mg/kg) every day for a total of eight days (Fig. 3E). Thirty minutes after the last injected, the mice were euthanized and different brain regions were dissected for further analysis of phosphorylation of MAPK/Akt pathways. The administration of methamphetamine significantly increased the phosphorylation of ERK, JNK, p38 and Akt in the hippocampus (Fig. 3D,E). These findings thus demonstrate that sigma-1 receptor-mediated ROS generation occurs upstream of methamphetamine-induced phosphorylation of the MAPK and PI3K/Akt cascades.

**Involvement of the MAPK and PI3K/Akt pathways in methamphetamine-induced translocation of STAT3 into the nucleus.** Mounting evidence suggests a link between STAT3 and inflammatory cytokines such as TNF- $\alpha$  and IL-6<sup>35,36</sup>. Thus, we next sought to examine whether methamphetamine-mediated microglial polarization involved the activation of STAT3. Methamphetamine increased STAT3 expression and concomitantly its translocation into the nucleus, with a maximal response within 30 min (Fig. 4A,B). Also, methamphetamine increased the expression of STAT3 in the cytoplasm (Fig. 4C). Consistent with the results of our studies described above, pretreating BV-2 cells with the STAT3 inhibitor stattic ameliorated the methamphetamine-mediated induction of M1 polarization from M2 phenotype of microglia (Fig. 4D,E). We next wanted to examine the functional role of upstream signaling pathways in the methamphetamine-mediated activation of STAT3. BV-2 cells were pretreated with inhibitors specific for various signaling pathways before they were stimulated with methamphetamine. Intriguingly, the JNK inhibitor SP600125, p38 inhibitor SB203580 and PI3K inhibitor LY294002, but not the MEK1/2 inhibitor U0126, significantly inhibited the methamphetamine-induced translocation of STAT3 (Fig. 4F,G). These findings thus link activation of the MAPK and PI3K/Akt pathways to the downstream translocation of STAT3 as well as to microglial polarization.

**Knockout of the sigma-1 receptor affected methamphetamine-induced microglial activation *in vivo*.** To better understand the role of the sigma-1 receptor in methamphetamine-induced microglial activation, mice were intraperitoneally injected with methamphetamine (30 mg/kg) every 2 h for a total of four injections. Twenty-four hours after the last injection, the mice were euthanized and different brain regions were dissected for further analysis of the expression of iNOS, Arginase and SOCS3. As an initial screening, we examined the effect of methamphetamine on microglial activation in different brain regions. The administration of methamphetamine significantly increased iNOS expression in the hippocampus, cerebellum, and midbrain (Fig. 5A–C,F–H) and down-regulated iNOS expression in the cortex and striatum (Fig. 5D,E,I,J).

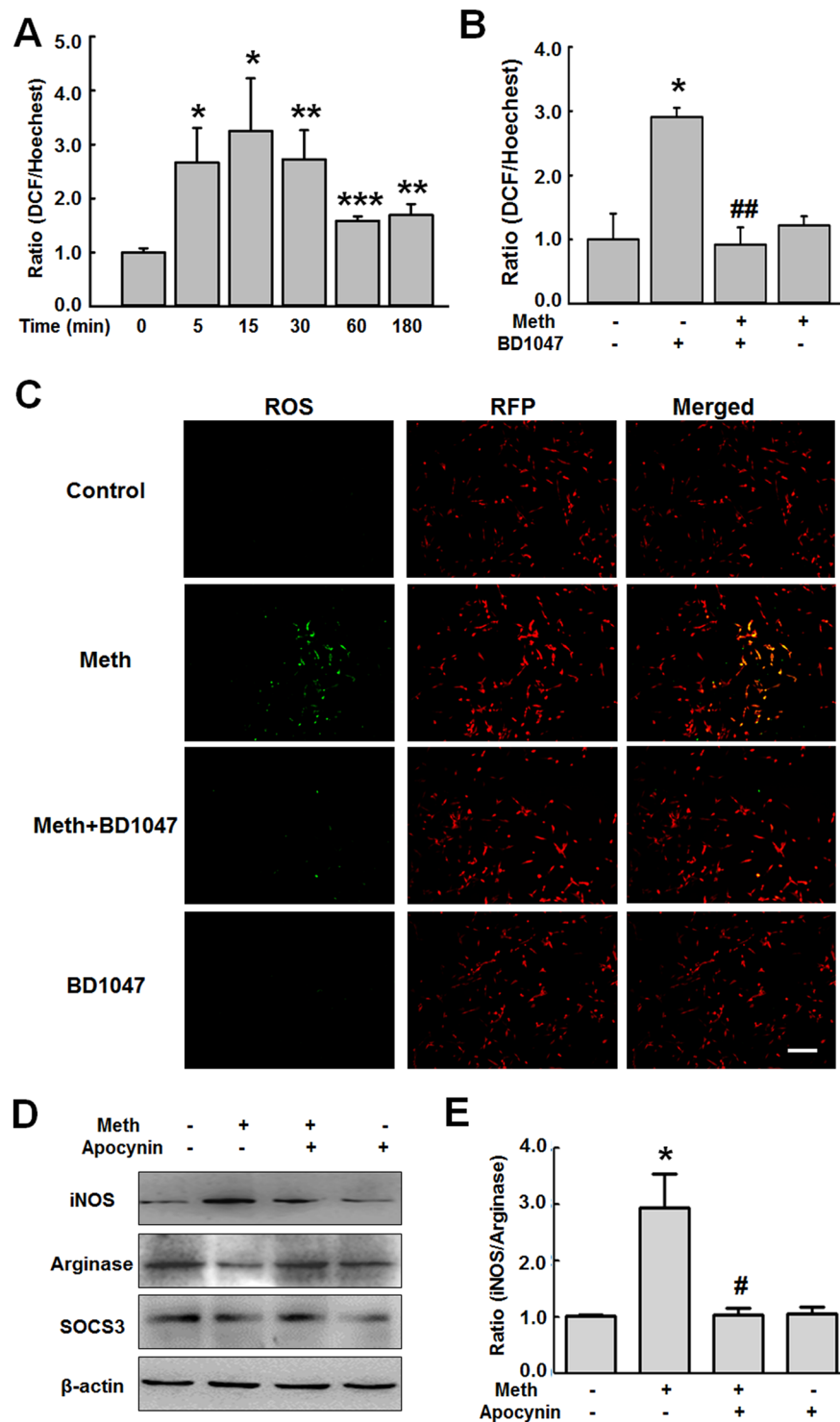


**Figure 2.** Methamphetamine induced ROS generation. (A) Reactive oxygen species (ROS) assay showing that methamphetamine (150  $\mu$ M) induced ROS generation in a time-dependent manner. \* $p < 0.05$ , \*\* $p < 0.01$ , \*\*\* $p < 0.001$  vs the control group using one-way ANOVA. (B) ROS assay showing that pretreatment of cells with the sigma-1 receptor inhibitor BD1047 attenuated the methamphetamine-induced ROS generation. \* $p < 0.05$  vs the control group; ## $p < 0.01$  vs the methamphetamine-treated group using one-way ANOVA. (C) Representative immunocytochemical images showing that BD1047 attenuated the methamphetamine-induced ROS generation. The ROS level was examined in BV-2 cells transduced with RFP-lentivirus. Green: DCF-DA; Red; RFP-lentivirus. Scale bar: 200  $\mu$ m. (D) Western blot showing that pretreatment with the NADPH inhibitor apocynin attenuated the methamphetamine-induced iNOS, arginase and SOCS3 expression in BV-2 cells. (E) Densitometric analyses of five separate experiments suggest that methamphetamine induced the ratio of iNOS and arginase expression, which was attenuated by apocynin pretreatment. \* $p < 0.05$  vs the control group; # $p < 0.05$  vs the methamphetamine-treated group using one-way ANOVA. Meth, methamphetamine.



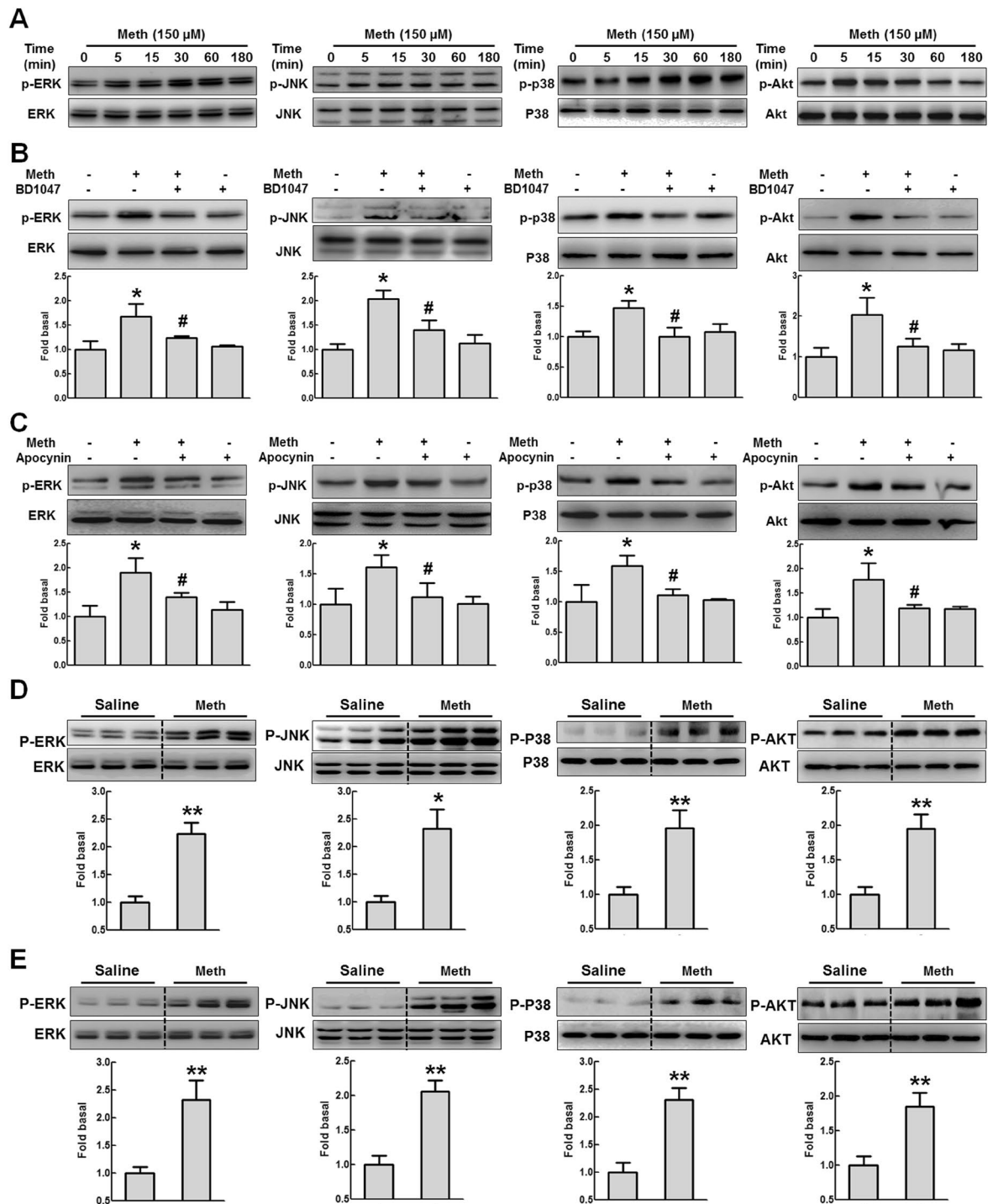


**Figure 3.** Methamphetamine induced the activation of the MAPK and PI3K/Akt pathways. **(A)** Representative western blot showing the effects of methamphetamine (150  $\mu$ M) on the phosphorylation of ERK, JNK, p38 and Akt in BV-2 cells. **(B)** Western blot and densitometric analyses showing that pretreatment with the sigma-1 receptor antagonist BD1047 attenuated the methamphetamine-induced phosphorylation of ERK, JNK, p38 and Akt in BV-2 cells. **(C)** Representative western blot and densitometric analyses showing the effects of apocynin on the methamphetamine-induced phosphorylation of ERK, JNK, p38 and Akt in BV-2 cells. \* $p < 0.05$  vs the control group; # $p < 0.05$  vs the methamphetamine-treated group using one-way ANOVA. **(D,E)** Representative western blot and densitometric analyses showed the effects of methamphetamine on the phosphorylation of ERK, JNK, p38 and Akt in the hippocampus. Mice were intraperitoneally injected with methamphetamine (30 mg/kg) every 2 h for a total of four injections **(D)** or with escalating dose methamphetamine (1.5 mg/kg, 4.5 mg/kg, 7.5 mg/kg, and 10 mg/kg) every day for a total of eight days **(E)**. Thirty minutes hours after the last injected, the mice were euthanized and the hippocampus was dissected for further analysis of phosphorylation of MAPK/Akt pathways. \* $p < 0.05$ , \*\* $p < 0.01$  vs the control group by Student's t-test. Meth, methamphetamine.

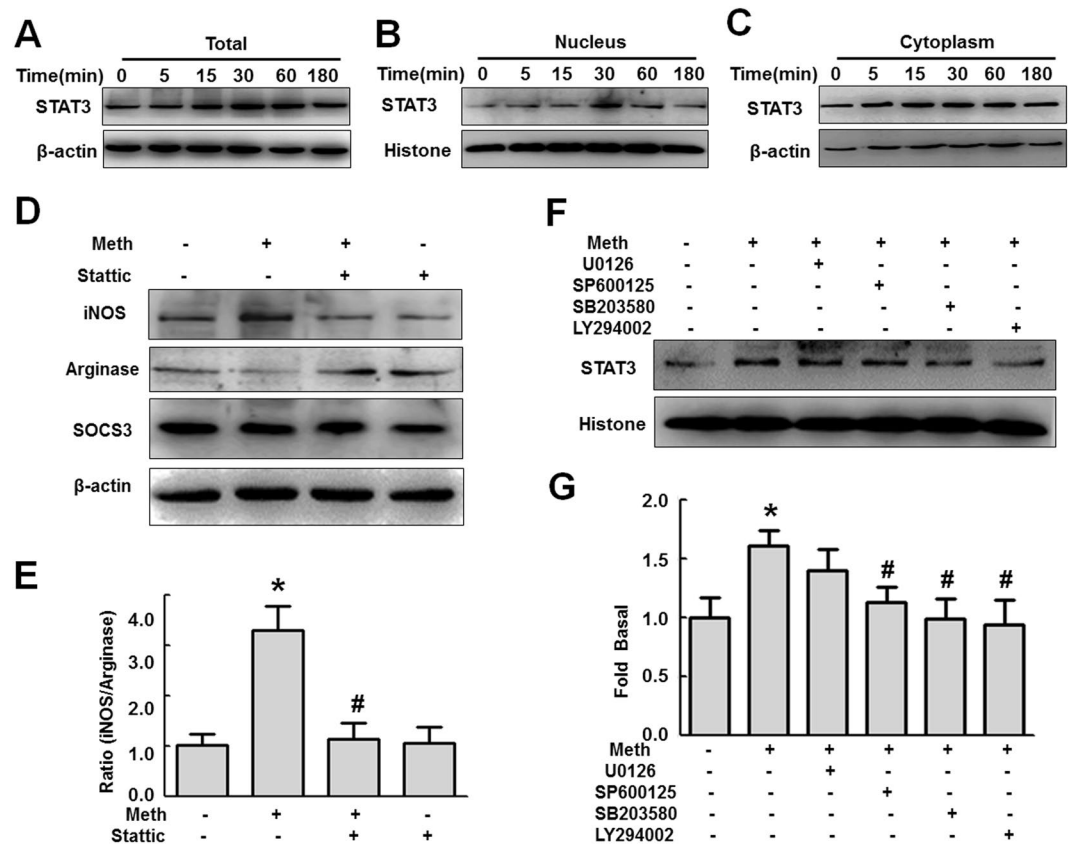


**Figure 4.** Involvement of the MAPK and PI3K/Akt pathways in the methamphetamine-induced translocation of STAT3 into the nucleus. (A–C) Representative western blot showing the effects of methamphetamine (150  $\mu$ M) on the expression of STAT in whole-cell lysates (A), nucleus (B) and cytoplasm (C) of BV-2 cells. (D) Representative western blot showing the effects of the STAT inhibitor static on the methamphetamine-induced the expression of iNOS, arginase and SOCS3 in BV-2 cells. (E) Densitometric analyses of five separate experiments suggest that Meth induced the ratio of iNOS and arginase expression, which was attenuated by static pretreatment. (F) Representative western blot showing that pretreatment with the ERK inhibitor (U0126, 10  $\mu$ M), p38 inhibitor (SP600125, 10  $\mu$ M), JNK inhibitor (SB203580, 10  $\mu$ M) and Akt inhibitor (LY294002, 10  $\mu$ M) affected the expression of STAT3 in BV-2 cells. (G) Densitometric analyses suggesting that methamphetamine induced STAT3 expression, which was attenuated by pretreatment with SP600125, SB203580 and LY294002 but not U0126. \* $p < 0.05$  vs the control group; # $p < 0.05$  vs the methamphetamine-treated group using two-way ANOVA. Meth, methamphetamine.

The hippocampal findings were consistent with the *in vitro* findings, so this brain region was chosen for all further *in vivo* studies.

In order to examine the role of sigma-1 receptor in microglial activation, microglial activation was examined in methamphetamine-injected sigma-1 receptor KO mice. WT and sigma-1 receptor KO mice were intraperitoneally injected with methamphetamine (30 mg/kg) every 2 h for a total of four injections. Twenty-four hours after the last injected, the mice were euthanized and hippocampal sections were immunostained for Iba-1. As shown in Fig. 6A–C, in the WT group, methamphetamine administration activated microglia in the hippocampus, as demonstrated by the significant increase in microglial soma size and concomitant decrease in cell processes. However, sigma-1 receptor deficiency significantly reduced methamphetamine-induced microglial activation (Fig. 6A–C). In order to further confirm the role of sigma-1 receptor in microglial activation, twenty-four hours after the last injected, the hippocampal brain region was dissected for further analysis of the expression of iNOS, Arginase and SOCS3. As shown in Fig. 6D, methamphetamine also increased iNOS expression in the hippocampus; this increase was significantly ameliorated in sigma-1 receptor KO mice, as quantified in Fig. 6E.

## Discussion

Although previous studies have demonstrated methamphetamine-induced microglial activation<sup>11, 12, 37</sup>, the molecular and cellular mechanisms involved in this process are not completely understood. Therefore, we demonstrated the vital role of the sigma-1 receptor in methamphetamine-mediated microglial activation *in vitro* and *in vivo*. The findings of the current study also illustrated the detailed mechanisms involved in sigma-1 receptor-mediated microglial activation, which involves ROS generation and the activation of the MAPK and PI3K/Akt pathways. Subsequent translocation of STAT3 then ultimately leads to microglial activation as summarized in Fig. 7.

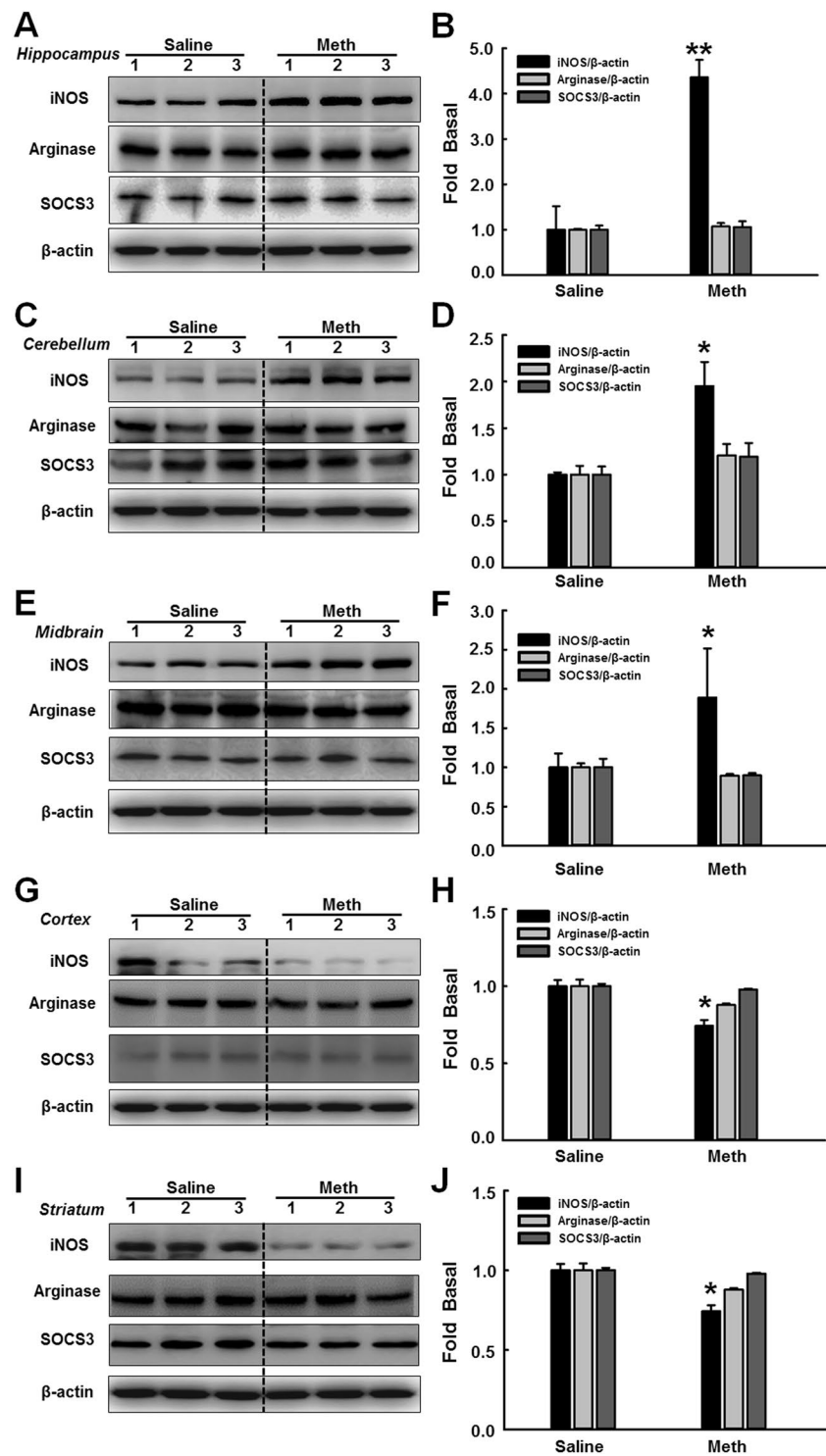


**Figure 5.** Involvement of the sigma-1 receptor in methamphetamine-induced microglial activation *in vivo*. (A–I) Representative western blot showing the effects of methamphetamine (30 mg/kg) on the expression of iNOS, arginase and SOCS3 in the hippocampus (A), cerebellum (C), midbrain (E), cortex (G) and striatum (I). (B–J) Densitometric analyses suggest that methamphetamine induced iNOS, arginase and SOCS3 expression in the hippocampus (B), cerebellum (D), midbrain (F), cortex (H) and striatum (J). Mice were intraperitoneally injected with methamphetamine (30 mg/kg) every 2 h for a total of four injections. Twenty-four hours after the last injected, the mice were euthanized and different brain regions were dissected for further analysis of the expression of iNOS, Arginase and SOCS3. N = 5 animals/group. \*p < 0.05, \*\*p < 0.01 vs the saline-treated group by Student's t-test. Meth, methamphetamine.



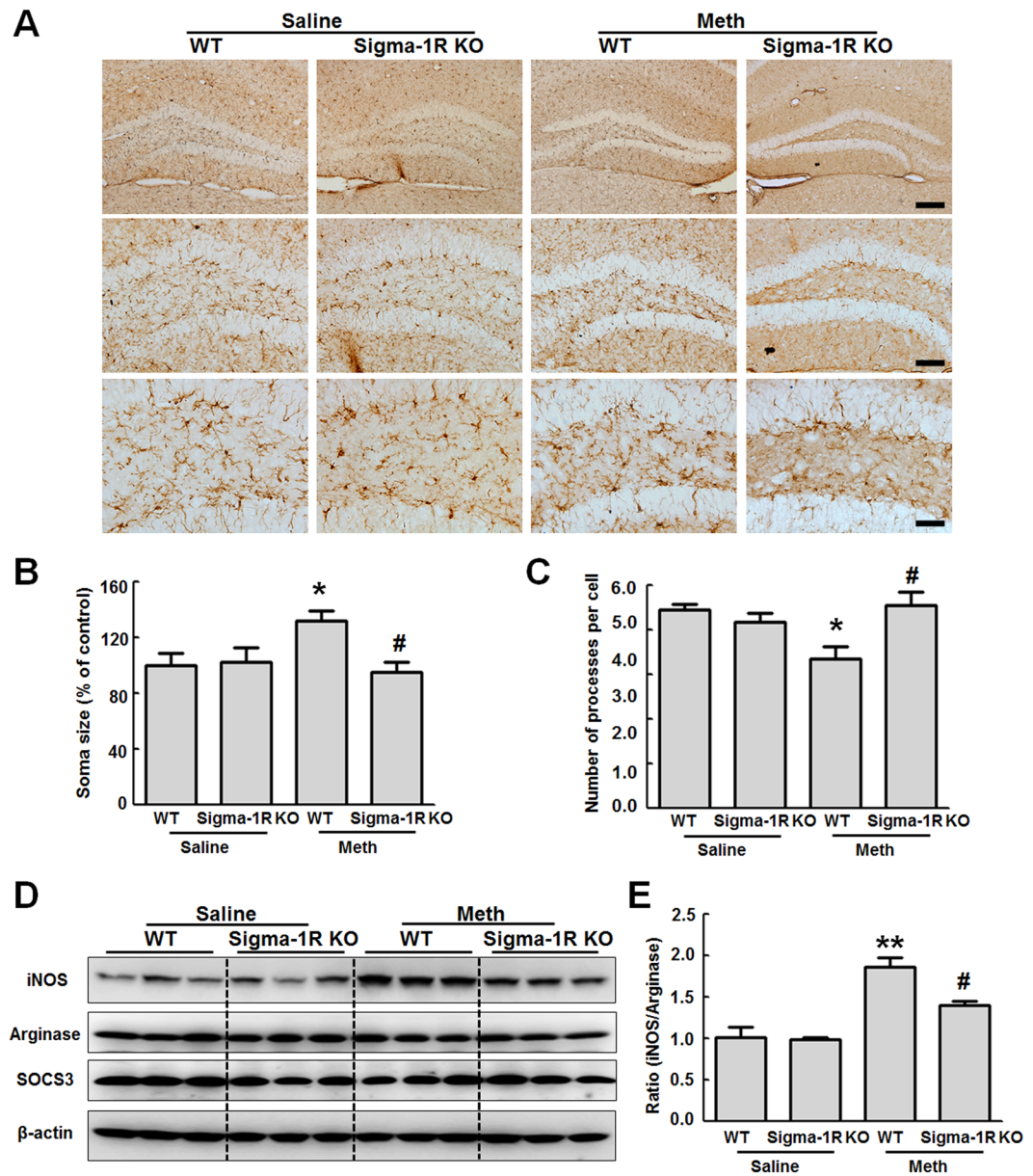


**Figure 6.** Knockout of the sigma-1 receptor affected methamphetamine-induced microglial activation *in vivo*. (A) Methamphetamine induced microglial activation in the hippocampus of WT and sigma-1 receptor KO mice. WT and sigma-1 receptor KO mice were intraperitoneally injected with methamphetamine (30 mg/kg) every 2 h for a total of four injections. Twenty-four hours after the last injected, the mice were euthanized and hippocampal sections were immunostained for Iba-1. Representative image of Iba-1 immunostaining in the hippocampus of mice injected with saline/methamphetamine. Scale bar: 200  $\mu\text{m}$  (upper panel), 100  $\mu\text{m}$  (middle panel), and 50  $\mu\text{m}$  (lower panel). (B,C) The soma size (B) and number of processes per cell (C) were quantified in the hippocampus of WT and sigma-1 receptor KO mice. (D) Representative western blot showing the effects of methamphetamine (30 mg/kg) on the expression of iNOS, arginase and SOCS3 in WT and sigma-1 receptor KO mice. (E) Densitometric analyses suggest that sigma-1 receptor KO mice attenuated methamphetamine-induced increased the ratio of iNOS and arginase expression in WT mice. WT and sigma-1 receptor KO mice were intraperitoneally injected with methamphetamine (30 mg/kg) every 2 h for a total of four injections. Twenty-four hours after the last injected, the mice were euthanized and hippocampal brain region was dissected for further analysis of the expression of iNOS, Arginase and SOCS3. N = 5 animals/group. \* $p < 0.05$ , \*\* $p < 0.01$  vs the saline-treated WT group; # $p < 0.05$  vs the methamphetamine-treated WT group using one-way ANOVA. Meth, methamphetamine. Sigma-1R: sigma-1 receptor.

Sigma receptors, non-opioid receptors, non-phencyclidine receptors, and intracellular receptors modulate multiple signal transduction and neurotransmitter systems. Two subtypes of sigma receptors, sigma-1 and sigma-2, have been identified<sup>38</sup>. The sigma-1 receptor is widely expressed in brain and peripheral tissues and has been

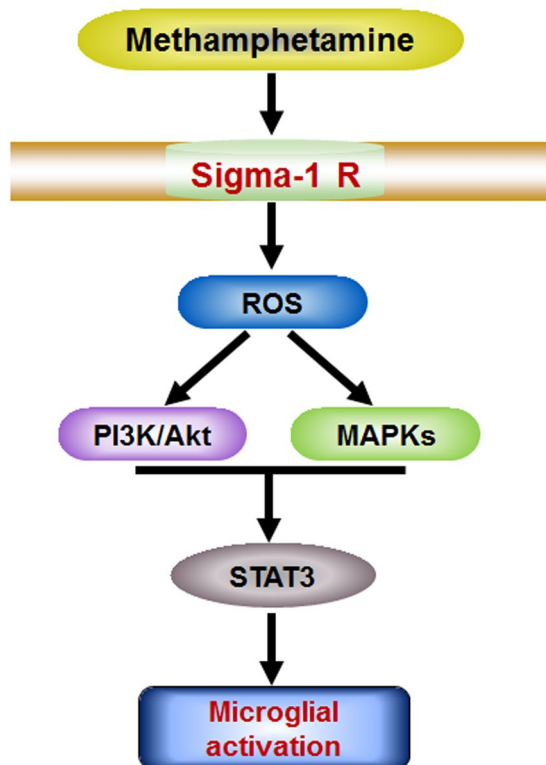


**Figure 7.** Schematic diagram showing the mechanisms underlying the involvement of the sigma-1 receptor in methamphetamine-induced microglial activation. Meth, methamphetamine. Sigma-1R: sigma-1 receptor.

localized to the plasma membrane as well as to intracellular structures such as the endoplasmic reticulum<sup>39,40</sup>. A variety of conditions have been associated with binding affinity for the sigma-1 receptor, including amnesia, schizophrenia<sup>41</sup>, cancer<sup>42</sup>, depression<sup>43</sup> and addiction<sup>44</sup>. Thus far, the contribution of the sigma-2 receptor remains poorly understood because of the paucity of available experimental tools to study the pathological and physiological processes in which it is involved. Consistent with previous studies<sup>23,45–47</sup>, inhibiting the sigma-1 receptor with the antagonist BD1047 significantly blocked methamphetamine-induced microglial polarization, implicating the sigma-1 receptor as a promising therapeutic candidate for the neuroinflammatory effects of methamphetamine. In addition, our *in vivo* study, in which we applied a genetic approach using the sigma-1 receptor KO animal model, further confirmed the finding that sigma-1 receptor blockage attenuated methamphetamine-induced microglial activation. However, in contrast to the methamphetamine-mediated microglial polarization we observed in our *in vitro* study, the expression of M2 phenotypic markers was not affected *in vivo*. This difference could be attributed to the fact that only macrophages/microglia were polarized, and this polarization was masked by other cells *in vivo*<sup>5,48</sup>. In addition, this difference could also be attributed to differences between the acute and late chronic phase of the methamphetamine model<sup>49</sup>. In this study, we also noticed that there was 50% effect reduced in sigma-1 receptor KO mice, whereas BD1047 abolished the ROS production induced by methamphetamine. This discrepancy maybe due to the fact that: 1) methamphetamine exerted its effect via other targets other than sigma-1 receptor; 2) it is possible for BD1047 to function beyond sigma-1 receptor due to the low specificity as a pharmacological approach.

A growing body of data continues to indicate that ROS play a crucial role in regulating myriad cellular signaling pathways. Moreover, accumulating studies have demonstrated that increased ROS is linked with microglial activation and the secretion of inflammatory factors, such as IL-1 $\beta$  and IL-18<sup>50–52</sup>. One of the mechanisms through which ROS are produced involves a respiratory burst orchestrated by the activation of NADPH oxidase<sup>53</sup>. Consistent with recent findings connecting NADPH oxidase activity with cytokine/chemokine production by microglia<sup>54,55</sup>, our findings clearly demonstrated that methamphetamine induced NADPH oxidase-generated ROS in a time-dependent manner and that the generated ROS played a critical role in microglial polarization. Interestingly, inhibiting BV-2 cells with BD1047 significantly attenuated the production of ROS induced by methamphetamine. This finding is in agreement with our previous study that showed that the sigma-1 receptor/lipid rafts played a critical role in NADPH-mediated ROS generation in cocaine-exposed microglial cells<sup>23</sup>, suggesting that sigma-1 receptor activation lies upstream of methamphetamine-mediated ROS generation.

We further examined the downstream signaling pathways involved in methamphetamine-induced microglial activation. Our present study revealed the involvement of phosphorylation of ERK, JNK, and the p38 MAPK and PI3K/Akt pathways in microglial activation mediated by methamphetamine. These findings are consistent with the effect of methamphetamine on the activation of the MAPK and PI3K/Akt pathways in human SH-SY5Y cells<sup>33</sup> and PC12 cells<sup>56</sup>. Mounting evidence suggests that low concentrations of ROS are important for the

regulation of pathways such as the TNF-ASK1 pathway<sup>57</sup>. Another key feature of our findings is that the activation of signaling pathways in this process depended on the formation of ROS, as demonstrated by the absence of methamphetamine-induced phosphorylation in the presence of the NADPH oxidase inhibitor apocynin; this result suggests that the activation of signaling pathways occurred downstream of methamphetamine-induced ROS generation.

STATs are involved in a series of biological events, including cell differentiation<sup>58</sup>, angiogenesis<sup>59</sup>, innate immunity<sup>60</sup> and cell growth regulation<sup>61</sup>. Numerous studies have demonstrated that STAT3 is mainly expressed in glial cells<sup>62,63</sup> and is involved in inflammatory reactions<sup>64,65</sup>. Our current study demonstrated that methamphetamine exposure induced time-dependent up-regulation of STAT3 protein and translocation of STAT3 into the nucleus. Similar to the results of our previous study described above, STAT3 blockage significantly ameliorated methamphetamine-mediated microglial activation. Further dissection of the signaling pathways involved in the methamphetamine-mediated translocation of STAT3 using a pharmacological approach revealed the involvement of the JNK, p38 and PI3K/Akt pathways but not of ERK. This finding is consistent with a previous study that showed that methamphetamine induced ERK phosphorylation; unfortunately, however, specific blockade of the ERK pathway failed to rescue the methamphetamine-induced death of SH-SY5Y cells<sup>33</sup>. Collectively, these results demonstrate that the MAPK and PI3K/Akt pathways lie upstream of STAT3.

Microglial activation is known to be a key feature of neuroinflammatory processes<sup>66,67</sup>. Activated microglia are characterized by a dynamic changing state, namely the classic M1 and alternative M2 activation. Our present study demonstrated that M1-M2 microglial polarization is a tightly controlled process that involves a set of signaling pathways and transcriptional regulatory networks. Our data provide the first evidence that the sigma-1 receptor plays a key role in methamphetamine-mediated microglial activation through the use of a genetic approach.

In summary, we detailed the molecular mechanisms associated with the dynamic changes involved in microglial polarization and provided evidence of their interactions; understanding of these interactions is crucial to elucidate the molecular basis of methamphetamine-induced disease progression and to design novel microglia-mediated therapeutic strategies.

**Declaration:.** The use of cell and animal was performed in accordance with the approved guidelines of the Research and Development Committee of Southeast University.

## References

- Krasnova, I. N., Justinova, Z. & Cadet, J. L. Methamphetamine addiction: involvement of CREB and neuroinflammatory signaling pathways. *Psychopharmacology* **233**, 1945–1962, doi:10.1007/s00213-016-4235-8 (2016).
- Saika, F., Kiguchi, N. & Kishioka, S. The role of CC-chemokine ligand 2 in the development of psychic dependence on methamphetamine. *Nihon Arukoru Yakubutsu Igakkai zasshi = Japanese journal of alcohol studies & drug dependence* **50**, 189–195 (2015).
- Harro, J. Neuropsychiatric adverse effects of amphetamine and methamphetamine. *International review of neurobiology* **120**, 179–204, doi:10.1016/bs.irn.2015.02.004 (2015).
- Sharma, H. S. & Kiyatkin, E. A. Rapid morphological brain abnormalities during acute methamphetamine intoxication in the rat: an experimental study using light and electron microscopy. *Journal of chemical neuroanatomy* **37**, 18–32, doi:10.1016/j.jchemneu.2008.08.002 (2009).
- Yao, H. *et al.* MiR-9 promotes microglial activation by targeting MCP1. *Nature communications* **5**, 4386, doi:10.1038/ncomms5386 (2014).
- Herrera, A. J. *et al.* Relevance of chronic stress and the two faces of microglia in Parkinson's disease. *Frontiers in cellular neuroscience* **9**, 312, doi:10.3389/fncel.2015.00312 (2015).
- Ma, Y., Wang, J., Wang, Y. & Yang, G. Y. The biphasic function of microglia in ischemic stroke. *Progress in neurobiology* <http://www.ncbi.nlm.nih.gov/pubmed/26851161> (2016).
- Yirmiya, R., Rimmerman, N. & Reshef, R. Depression as a microglial disease. *Trends in neurosciences* **38**, 637–658, doi:10.1016/j.tins.2015.08.001 (2015).
- Sekine, Y. *et al.* Methamphetamine causes microglial activation in the brains of human abusers. *The Journal of neuroscience: the official journal of the Society for Neuroscience* **28**, 5756–5761, doi:10.1523/JNEUROSCI.1179-08.2008 (2008).
- Robson, M. J. *et al.* SN79, a sigma receptor ligand, blocks methamphetamine-induced microglial activation and cytokine upregulation. *Experimental neurology* **247**, 134–142, doi:10.1016/j.expneurol.2013.04.009 (2013).
- McConnell, S. E., O'Banion, M. K., Cory-Slechta, D. A., Olschowka, J. A. & Opanashuk, L. A. Characterization of binge-dosed methamphetamine-induced neurotoxicity and neuroinflammation. *Neurotoxicology* **50**, 131–141, doi:10.1016/j.neuro.2015.08.006 (2015).
- Fernandes, N. C. *et al.* Methamphetamine alters microglial immune function through P2X7R signaling. *Journal of neuroinflammation* **13**, 91, doi:10.1186/s12974-016-0553-3 (2016).
- Heneka, M. T., Kummer, M. P. & Latz, E. Innate immune activation in neurodegenerative disease. *Nature reviews. Immunology* **14**, 463–477, doi:10.1038/nri3705 (2014).
- Meireles, M. *et al.* Anthocyanin effects on microglia M1/M2 phenotype: consequence on neuronal fractalkine expression. *Behavioural brain research* **305**, 223–228, doi:10.1016/j.bbr.2016.03.010 (2016).
- De Simone, R. *et al.* The mitochondrial uncoupling protein-2 is a master regulator of both M1 and M2 microglial responses. *Journal of neurochemistry* **135**, 147–156, doi:10.1111/jnc.13244 (2015).
- Bowen, W. D., Hellewell, S. B. & McGarry, K. A. Evidence for a multi-site model of the rat brain sigma receptor. *European journal of pharmacology* **163**, 309–318 (1989).
- Urfer, R. *et al.* Phase II trial of the Sigma-1 receptor agonist cutamesine (SA4503) for recovery enhancement after acute ischemic stroke. *Stroke; a journal of cerebral circulation* **45**, 3304–3310, doi:10.1161/STROKEAHA.114.005835 (2014).
- Diaz, J. L. *et al.* Synthesis and structure-activity relationship study of a new series of selective sigma(1) receptor ligands for the treatment of pain: 4-aminotriazoles. *Journal of medicinal chemistry* **58**, 2441–2451, doi:10.1021/jm501920g (2015).
- Roth, M. D., Whittaker, K. M., Choi, R., Tashkin, D. P. & Baldwin, G. C. Cocaine and sigma-1 receptors modulate HIV infection, chemokine receptors, and the HPA axis in the huPBL-SCID model. *Journal of leukocyte biology* **78**, 1198–1203, doi:10.1189/jlb.0405219 (2005).
- Guo, L. & Zhen, X. Sigma-2 receptor ligands: neurobiological effects. *Current medicinal chemistry* **22**, 989–1003 (2015).
- Smith, K. J., Butler, T. R. & Prendergast, M. A. Inhibition of sigma-1 receptor reduces N-methyl-D-aspartate induced neuronal injury in methamphetamine-exposed and -naive hippocampi. *Neuroscience letters* **481**, 144–148, doi:10.1016/j.neulet.2010.06.069 (2010).



22. Yasui, Y. & Su, T. P. Potential molecular mechanisms on the role of the sigma-1 receptor in the action of cocaine and methamphetamine. *Journal of drug and alcohol research* **5** <http://www.ncbi.nlm.nih.gov/pubmed/27088037> (2016).
23. Yao, H. *et al.* Molecular mechanisms involving sigma receptor-mediated induction of MCP-1: implication for increased monocyte transmigration. *Blood* **115**, 4951–4962, doi:10.1182/blood-2010-01-266221 (2010).
24. Bai, Y. *et al.* Silencing microRNA-143 protects the integrity of the blood-brain barrier: implications for methamphetamine abuse. *Scientific reports* **6**, 35642, doi:10.1038/srep35642 (2016).
25. Chao, J. *et al.* Expression of green fluorescent protein in human foreskin fibroblasts for use in 2D and 3D culture models. *Wound Repair Regen* **22**, 134–140, doi:10.1111/wrr.12121 (2014).
26. Liu, H. *et al.* Macrophage-derived MCP1P1 mediates silica-induced pulmonary fibrosis via autophagy. *Part Fibre Toxicol* **13**, 55, doi:10.1186/s12989-016-0167-z.
27. Zhang, Y. *et al.* Role of high-mobility group box 1 in methamphetamine-induced activation and migration of astrocytes. *Journal of neuroinflammation* **12**, 156, doi:10.1186/s12974-015-0374-9 (2015).
28. Liu, H. *et al.* MCP1P1 mediates silica-induced cell migration in human pulmonary fibroblasts. *Am J Physiol Lung Cell Mol Physiol* **310**, L121–132, doi:10.1152/ajplung.00278.2015.
29. Seminerio, M. J., Robson, M. J., McCurdy, C. R. & Matsumoto, R. R. Sigma receptor antagonists attenuate acute methamphetamine-induced hyperthermia by a mechanism independent of IL-1beta mRNA expression in the hypothalamus. *European journal of pharmacology* **691**, 103–109, doi:10.1016/j.ejphar.2012.07.029 (2012).
30. Zhang, Y. *et al.* Involvement of sigma-1 receptor in astrocyte activation induced by methamphetamine via up-regulation of its own expression. *Journal of neuroinflammation* **12**, 29, doi:10.1186/s12974-015-0250-7 (2015).
31. Riddle, E. L., Fleckenstein, A. E. & Hanson, G. R. Mechanisms of methamphetamine-induced dopaminergic neurotoxicity. *The AAPS journal* **8**, E413–418 (2006).
32. Gonzalez, B. *et al.* Modafinil improves methamphetamine-induced object recognition deficits and restores prefrontal cortex ERK signaling in mice. *Neuropharmacology* **87**, 188–197, doi:10.1016/j.neuropharm.2014.02.002 (2014).
33. Wang, S. F., Yen, J. C., Yin, P. H., Chi, C. W. & Lee, H. C. Involvement of oxidative stress-activated JNK signaling in the methamphetamine-induced cell death of human SH-SY5Y cells. *Toxicology* **246**, 234–241, doi:10.1016/j.tox.2008.01.020 (2008).
34. Ma, J. *et al.* Methamphetamine induces autophagy as a pro-survival response against apoptotic endothelial cell death through the Kappa opioid receptor. *Cell death & disease* **5**, e1099, doi:10.1038/cddis.2014.64 (2014).
35. Valdez, I. A. *et al.* Proinflammatory cytokines induce endocrine differentiation in pancreatic ductal cells via STAT3-dependent NGN3 activation. *Cell reports* **15**, 460–470, doi:10.1016/j.celrep.2016.03.036 (2016).
36. Zimmers, T. A., Fishel, M. L. & Bonetto, A. STAT3 in the systemic inflammation of cancer cachexia. *Seminars in cell & developmental biology* **54**, 28–41, doi:10.1016/j.semcdb.2016.02.009 (2016).
37. Shin, E. J. *et al.* Ginsenoside Re rescues methamphetamine-induced oxidative damage, mitochondrial dysfunction, microglial activation, and dopaminergic degeneration by inhibiting the protein kinase Cdelta gene. *Molecular neurobiology* **49**, 1400–1421, doi:10.1007/s12035-013-8617-1 (2014).
38. Hanner, M. *et al.* Purification, molecular cloning, and expression of the mammalian sigma1-binding site. *Proceedings of the National Academy of Sciences of the United States of America* **93**, 8072–8077 (1996).
39. McCann, D. J., Weissman, A. D. & Su, T. P. Sigma-1 and sigma-2 sites in rat brain: comparison of regional, ontogenetic, and subcellular patterns. *Synapse* **17**, 182–189, doi:10.1002/syn.890170307 (1994).
40. Alonso, G. *et al.* Immunocytochemical localization of the sigma(1) receptor in the adult rat central nervous system. *Neuroscience* **97**, 155–170 (2000).
41. Karantinos, T. *et al.* Increased intra-subject reaction time variability in the volitional control of movement in schizophrenia. *Psychiatry research* **215**, 26–32, doi:10.1016/j.psychres.2013.10.031 (2014).
42. Aydar, E., Stratton, D., Fraser, S. P., Djamgoz, M. B. & Palmer, C. Sigma-1 receptors modulate neonatal Na1.5 ion channels in breast cancer cell lines. *European biophysics journal: EBJ* <http://www.ncbi.nlm.nih.gov/pubmed/27160185> (2016).
43. Lenart, L. *et al.* The role of sigma-1 receptor and brain-derived neurotrophic factor in the development of diabetes and comorbid depression in streptozotocin-induced diabetic rats. *Psychopharmacology* **233**, 1269–1278, doi:10.1007/s00213-016-4209-x (2016).
44. Katz, J. L., Hong, W. C., Hiranita, T. & Su, T. P. A role for sigma receptors in stimulant self-administration and addiction. *Behavioural pharmacology* **27**, 100–115, doi:10.1097/FBP.0000000000000209 (2016).
45. Zhang, Y. *et al.* Involvement of sigma-1 receptor in astrocyte activation induced by methamphetamine via up-regulation of its own expression. *Journal of neuroinflammation* **12**, 29, doi:10.1186/s12974-015-0250-7 (2015).
46. Zhang, Y. *et al.* Role of high-mobility group box 1 in methamphetamine-induced activation and migration of astrocytes. *Journal of neuroinflammation* **12**, 156, doi:10.1186/s12974-015-0374-9 (2015).
47. Yao, H., Duan, M. & Buch, S. Cocaine-mediated induction of platelet-derived growth factor: implication for increased vascular permeability. *Blood* **117**, 2538–2547, doi:10.1182/blood-2010-10-313593 (2011).
48. Kroner, A. *et al.* TNF and increased intracellular iron alter macrophage polarization to a detrimental M1 phenotype in the injured spinal cord. *Neuron* **83**, 1098–1116, doi:10.1016/j.neuron.2014.07.027 (2014).
49. Benson, M. J., Manzanero, S. & Borges, K. Complex alterations in microglial M1/M2 markers during the development of epilepsy in two mouse models. *Epilepsia* **56**, 895–905, doi:10.1111/epi.12960 (2015).
50. Liao, K. *et al.* Cocaine-mediated induction of microglial activation involves the ER stress-TLR2 axis. *Journal of neuroinflammation* **13**, 33, doi:10.1186/s12974-016-0501-2 (2016).
51. Shi, J. X., Wang, Q. J., Li, H. & Huang, Q. Silencing of USP22 suppresses high glucose-induced apoptosis, ROS production and inflammation in podocytes. *Molecular bioSystems* **12**, 1445–1456, doi:10.1039/c5mb00722d (2016).
52. Li, X. *et al.* Helicobacter pylori induces IL-1beta and IL-18 production in human monocytic cell line through activation of NLRP3 inflammasome via ROS signaling pathway. *Pathogens and disease* **73** <http://www.ncbi.nlm.nih.gov/pubmed/25834143> (2015).
53. Williams, R. *et al.* Cooperative induction of CXCL10 involves NADPH oxidase: Implications for HIV dementia. *Glia* **58**, 611–621, doi:10.1002/glia.20949 (2010).
54. Turchan-Cholewo, J. *et al.* Morphine and HIV-Tat increase microglial-free radical production and oxidative stress: possible role in cytokine regulation. *Journal of neurochemistry* **108**, 202–215, doi:10.1111/j.1471-4159.2008.05756.x (2009).
55. Turchan-Cholewo, J. *et al.* NADPH oxidase drives cytokine and neurotoxin release from microglia and macrophages in response to HIV-Tat. *Antioxidants & redox signaling* **11**, 193–204, doi:10.1089/ARS.2008.2097 (2009).
56. Wu, J. *et al.* Lithium protects against methamphetamine-induced neurotoxicity in PC12 cells via Akt/GSK3beta/mTOR pathway. *Biochemical and biophysical research communications* **465**, 368–373, doi:10.1016/j.bbrc.2015.08.005 (2015).
57. Ishaq, M. *et al.* Atmospheric gas plasma-induced ROS production activates TNF-ASK1 pathway for the induction of melanoma cancer cell apoptosis. *Molecular biology of the cell* **25**, 1523–1531, doi:10.1091/mbc.E13-10-0590 (2014).
58. Haricharan, S. & Li, Y. STAT signaling in mammary gland differentiation, cell survival and tumorigenesis. *Molecular and cellular endocrinology* **382**, 560–569, doi:10.1016/j.mce.2013.03.014 (2014).
59. Yang, X. & Friedl, A. A positive feedback loop between prolactin and STAT5 promotes angiogenesis. *Advances in experimental medicine and biology* **846**, 265–280, doi:10.1007/978-3-319-12114-7\_12 (2015).
60. Hillmer, E. J., Zhang, H., Li, H. S. & Watowich, S. S. STAT3 signaling in immunity. *Cytokine & growth factor reviews* <http://www.ncbi.nlm.nih.gov/pubmed/27185365> (2016).

61. Sun, G. & Irvine, K. D. Control of growth during regeneration. *Current topics in developmental biology* **108**, 95–120, doi:[10.1016/B978-0-12-391498-9.00003-6](https://doi.org/10.1016/B978-0-12-391498-9.00003-6) (2014).
62. Liu, S. *et al.* Spinal IL-33/ST2 signaling contributes to neuropathic pain via neuronal CaMKII-CREB and astroglial JAK2-STAT3 cascades in mice. *Anesthesiology* **123**, 1154–1169, doi:[10.1097/ALN.0000000000000850](https://doi.org/10.1097/ALN.0000000000000850) (2015).
63. LeComte, M. D., Shimada, I. S., Sherwin, C. & Spees, J. L. Notch1-STAT3-ETBR signaling axis controls reactive astrocyte proliferation after brain injury. *Proceedings of the National Academy of Sciences of the United States of America* **112**, 8726–8731, doi:[10.1073/pnas.1501029112](https://doi.org/10.1073/pnas.1501029112) (2015).
64. Muhl, H. STAT3, a key parameter of cytokine-driven tissue protection during sterile inflammation - the case of experimental acetaminophen (paracetamol)-induced liver damage. *Frontiers in immunology* **7**, 163, doi:[10.3389/fimmu.2016.00163](https://doi.org/10.3389/fimmu.2016.00163) (2016).
65. Deguchi, A. Curcumin targets in inflammation and cancer. *Endocrine, metabolic & immune disorders drug targets* **15**, 88–96 (2015).
66. Xiong, X. Y., Liu, L. & Yang, Q. W. Functions and mechanisms of microglia/macrophages in neuroinflammation and neurogenesis after stroke. *Progress in neurobiology* <http://www.ncbi.nlm.nih.gov/pubmed/27166859> (2016).
67. Yuan, Y., Fang, M., Wu, C. Y. & Ling, E. A. Scutellarin as a potential therapeutic agent for microglia-mediated neuroinflammation in cerebral ischemia. *Neuromolecular medicine* <http://www.ncbi.nlm.nih.gov/pubmed/27103430> (2016).

### Author Contributions

J.C. designed and performed the experiments, interpreted the data, prepared the figures, and wrote the manuscript. Y.Z. and L.D. performed the experiments and interpreted the data. R.Z., X.W. and K.S. designed the experiments, interpreted the data, and wrote the manuscript. H.Y. provided laboratory space and funding, designed the experiments, interpreted the data, wrote the manuscript, and directed the project. All authors read, commented on, and approved the final manuscript.

### Additional Information

**Competing Interests:** The authors declare that they have no competing interests.

**Publisher's note:** Springer Nature remains neutral with regard to jurisdictional claims in published maps and institutional affiliations.



**Open Access** This article is licensed under a Creative Commons Attribution 4.0 International License, which permits use, sharing, adaptation, distribution and reproduction in any medium or format, as long as you give appropriate credit to the original author(s) and the source, provide a link to the Creative Commons license, and indicate if changes were made. The images or other third party material in this article are included in the article's Creative Commons license, unless indicated otherwise in a credit line to the material. If material is not included in the article's Creative Commons license and your intended use is not permitted by statutory regulation or exceeds the permitted use, you will need to obtain permission directly from the copyright holder. To view a copy of this license, visit <http://creativecommons.org/licenses/by/4.0/>.

© The Author(s) 2017